

The dynamics of a doped hole in cuprates is not controlled by spin fluctuations

Hadi Ebrahimnejad,¹ George A. Sawatzky,^{1,2} and Mona Berciu^{1,2}

¹*Department of Physics and Astronomy, University of British Columbia, Vancouver B.C. V6T 1Z1, Canada*

²*Quantum Matter Institute, University of British Columbia, Vancouver B.C. V6T 1Z4, Canada*

Twenty seven years after the discovery of high-temperature superconductivity [1], consensus on its theoretical explanation is still absent. To a good extent, this is due to the difficulty of studying strongly correlated systems near half-filling, needed to understand the behaviour of one or few holes doped into a CuO_2 layer. To simplify this task it is customary to replace three-band models [2] describing the doping holes as entering the O $2p$ orbitals of these charge-transfer insulators [3] with much simpler one-band Hubbard or tJ models [4, 5]. Here we challenge this approach, showing that not only is the dynamics of a doped hole easier to understand in models that explicitly include the O orbitals, but also that our solution contradicts the long-held belief that the quantum spin fluctuations of the antiferromagnetic (AFM) background play a key role in determining this dynamics. Indeed, we show that the correct, experimentally observed dispersion is generically obtained for a hole moving on the O sublattice, and coupled to a Néel lattice of spins without spin fluctuations. This marks a significant conceptual change in our understanding of the relevant phenomenology and opens the way to studying few-holes dynamics without finite-size effect issues [6], to understand the actual strength of the “magnetic glue”.

The simplification from three-band to one-band models is based on the idea that the quasiparticle resulting when one hole is doped in the system has predominantly Zhang-Rice singlet (ZRS) character [7, 8]. Agreement between the quasiparticle dispersion for a generalized tJ model (with longer range hopping) and that measured by angle-resolved photoemission spectroscopy (ARPES) in parent compounds [9–14] is taken as evidence that one-band models are valid. Whether this is a good approximation in all the Brillouin zone and also for finite doping, or whether it is valid only near the $(\frac{\pi}{2}, \frac{\pi}{2})$ minimum, is still debated [15]. In one-band models, moreover, spin- and charge-fluctuations arise from the same particle-hole excitations, making it difficult to envisage a separation between the quasiparticles and the pairing glue. Such a separation, however, is assumed in most theories describing spin-fluctuations mediated pairing [4]. Even more problematic are recent arguments that such a strong attractive interaction mediated by spin-fluctuations is actually ignored by one-band models [16]. In other words, even if these models capture the quasiparticle dispersion

accurately, they may still fail to properly describe their effective interactions.

To fully answer these questions, one needs to be able to compare predictions of the three-band and one-band models not just in the single hole sector, where a single quasiparticle forms and its dispersion can be calculated, but also in the two-hole sector, where the effective interactions between quasiparticles can be studied. Carrying out two-hole calculations by exact numerical means is still too difficult a task: quantum Monte Carlo algorithms suffer from sign problems, while at present exact diagonalization (ED) can be carried out only on rather small clusters, where the finite size effects are still considerable and render the interpretation of the results difficult [6].

In this Article we show that a simple variational approximation for a three-band model on an infinite lattice captures all main known aspects of the quasiparticle behavior not just qualitatively, but also quantitatively. This approximation can also be systematically improved by increasing the variational space; this provides an estimate for the relevance of the excluded states. Most importantly, this method can be straightforwardly generalized to calculate few-hole propagators [16, 17].

Here we present the one-hole solution which already reveals several major surprises: (i) we find that the spin fluctuations of the AFM background play a negligible role in determining the quasiparticle dispersion, because the hole moves on a different sublattice. By contrast, in one-band models it is widely believed that the dynamics of a ZRS is controlled by these fluctuations, because not only does the ZRS move in the magnetic sublattice but it is also a coherent mix of spin and charge degrees of freedom. We argue that this view is wrong, and that the necessary inclusion of longer-range hopping in one-band models has precisely the effect of minimizing the role of the spin fluctuations; (ii) the quasiparticle’s dispersion in our model has the characteristic shape measured experimentally for any reasonable choice of parameters, unlike in one-band models where addition of longer range hoppings is necessary to obtain the correct dispersion, as mentioned above; (iii) our method allows us to study five-band models to understand the importance of the in-plane O $2p$ orbitals which do not hybridize directly with Cu $3d_{x^2-y^2}$. While, as expected, we find that the quasiparticle dispersion is little affected, the ARPES spectral weight is significantly changed and now exhibits a strong suppression outside the magnetic Brillouin zone in agreement with ARPES findings [9, 13]. This suggests that even three-band mod-

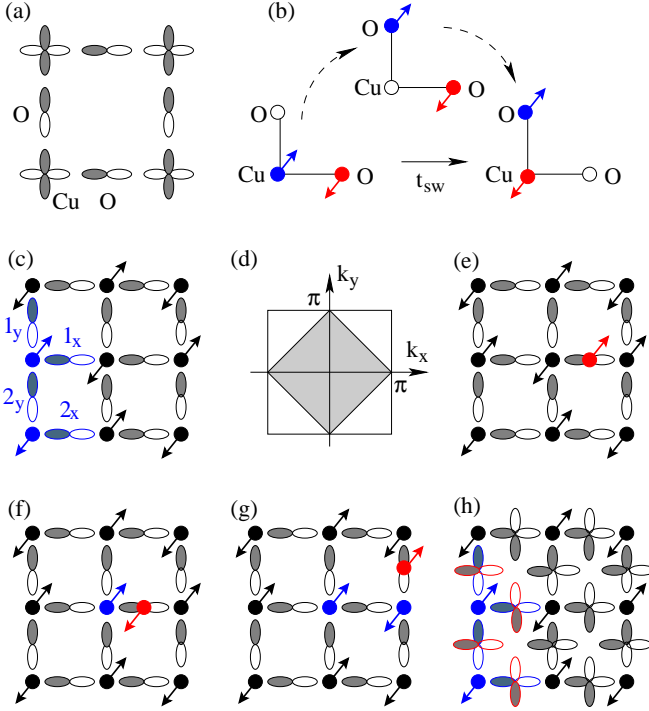


FIG. 1: (a) Sketch of three-band model which includes the Cu $3d_{x^2-y^2}$ and the O ligand $2p_{x/y}$ orbitals. White/shaded areas indicate our choice for the positive/negative lobes; (b) Sketch of a spin-swap process which results in effective hopping of the hole while its spin is swapped with that of the neighbour Cu; (c) Unit cell for Néel AFM order, consisting of two Cu spins and four O orbitals (highlighted in blue); (d) Magnetic Brillouin zone (shaded area) and the full Brillouin zone; (e) Example of a zero-magnon configuration, with the spin-up hole on an O orbital (red arrow) and the Cu spins with Néel order; (f) Example of a one-magnon configuration, where a Cu spin (marked in blue) is flipped, as is the hole's spin (red arrow); (g) Example of a two-magnon configuration, with two flipped Cu spins (shown in blue). The hole is spin-up again (red arrow); (h) Unit cell for Néel AFM order in the five-band model. The additional O orbitals are highlighted in red.

els do not fully capture all the quasiparticle properties.

The model we study can be thought of as the tJ analog of the three-band Emery model [2]: double-occupancy on the Cu sites is forbidden because of the large on-site Hubbard repulsion, so there is a spin- $\frac{1}{2}$ at each Cu site while the doping hole enters the O $2p$ ligand orbitals, see Figs. 1(a),(e). The resulting Hamiltonian is [15]:

$$\mathcal{H} = T_{pp} + T_{swap} + H_{J_{pd}} + H_{J_{dd}}. \quad (1)$$

T_{pp} describes first and second nearest neighbour (nn) hopping of the hole; T_{swap} describes effective hopping of the hole mediated by the Cu spin, whereby first the Cu hole hops onto a neighbour O followed then by the original hole filling the Cu orbital, see Fig. 1(b). Note that this leads to a swap of the spins of the hole and the Cu; $H_{J_{pd}}$ describes the AFM exchange between the spins of the hole and of its two neighbour Cu; and $H_{J_{dd}}$

describes the nn AFM superexchange between Cu spins except on the bond occupied by the hole. If $J_{dd} = 1$ is the energy unit, then $t_{pp} = 4.13$, $t'_{pp} = 2.40$, $t_{sw} = 2.98$ and $J_{pd} = 2.83$, respectively. The reader is referred to Ref. [15] for further details on the Hamiltonian, and on its ED solution for a hole on a 32 Cu + 64 O cluster.

In order to study this Hamiltonian on an infinite lattice, we make the key simplification of reducing $H_{J_{dd}}$ to an Ising form, instead of its full Heisenberg form. As a result, the undoped ground-state |AFM⟩ is a simple Néel state without any spin-fluctuations. This approach will be justified *a posteriori* based on the results it leads to.

The unit cell of the Néel AFM has two Cu spins and thus four distinct O sites; this and the corresponding magnetic Brillouin zone (MBZ) are shown in Figs. 1(c),(d). Thus, there are four inequivalent hole Bloch states $p_{\mathbf{k},\alpha,\sigma}^\dagger = \frac{1}{\sqrt{N}} \sum_{i \in A_\alpha} e^{i\mathbf{k}\cdot\mathbf{R}_{i,\alpha}} p_{i,\alpha,\sigma}^\dagger$, where $N \rightarrow \infty$ is the number of unit cells, $\alpha \in \{1_x, 1_y, 2_x, 2_y\}$ labels the type of O orbital while A_α is the sublattice of all O of type α , $\mathbf{R}_{i,\alpha}$ is the location of the α O of unit cell i , \mathbf{k} is a quasi-momentum inside the MBZ and $p_{i,\alpha,\sigma}^\dagger$ creates a spin- σ hole at $O_{i,\alpha}$. In the following we set $\sigma = \uparrow$ (the $\sigma = \downarrow$ case is treated similarly and gives identical results) and define the single-hole propagators:

$$G_{\beta\alpha}(\mathbf{k}, \omega) = \langle \text{AFM} | p_{\mathbf{k},\beta,\uparrow} \hat{G}(\omega) p_{\mathbf{k},\alpha,\uparrow}^\dagger | \text{AFM} \rangle \quad (2)$$

where $\hat{G}(\omega) = [\omega + i\eta - \mathcal{H}]^{-1}$, $\hbar = 1$ and $\eta > 0$ is a small broadening. The energy ω is measured from the undoped ground-state, i.e. we set $\mathcal{H}_{J_{dd}} | \text{AFM} \rangle = 0$. The one-hole spectrum $E_n(\mathbf{k})$ is given by the poles of these propagators, while from the residues one can find the overlaps $\langle n, \mathbf{k}, \uparrow | p_{\mathbf{k},\alpha,\uparrow}^\dagger | \text{AFM} \rangle$, where $\mathcal{H} | n, \mathbf{k}, \uparrow \rangle = E_n(\mathbf{k}) | n, \mathbf{k}, \uparrow \rangle$ are the one-hole eigenstates for band n .

To calculate these propagators, we use the identity $\hat{G}(\omega)(\omega + i\eta - \mathcal{H}) = 1$ to find $(\omega + i\eta)G_{\beta\alpha}(\mathbf{k}, \omega) = \delta_{\alpha,\beta} + \langle \text{AFM} | p_{\mathbf{k},\beta,\uparrow} \hat{G}(\omega) \mathcal{H} p_{\mathbf{k},\alpha,\uparrow}^\dagger | \text{AFM} \rangle$. The Hamiltonian has (i) terms which do not change either the hole location or its spin ($\mathcal{H}_{J_{dd}}$ and the diagonal part of $\mathcal{H}_{J_{pd}}$) and lead to a simple energy shift; (ii) terms which change the hole location but not its spin (T_{pp} and terms in T_{swap} which move the hole past the Cu with the same spin orientation) and link $G_{\beta\alpha}$ to other $G_{\beta'\alpha'}$; and (iii) terms which flip the hole's spin, while also flipping a neighbouring Cu spin (terms in T_{swap} which move the hole past the Cu with antiparallel spin, and the off-diagonal part of $\mathcal{H}_{J_{pd}}$). These last terms define generalized propagators which we call one-magnon propagators because they are projected on states that have a magnon (flipped Cu spin) beside the hole. One example of such a state is shown in Fig. 1(f). Equations of motion for the one-magnon propagators are obtained similarly, and link them to other one-magnon propagators with a different hole-magnon distance, to two-magnon propagators like shown in Fig. 1(g), since the hole can flip a second Cu spin, and – if the hole and magnon are on neighbouring sites – back to various $G_{\beta\alpha}$.

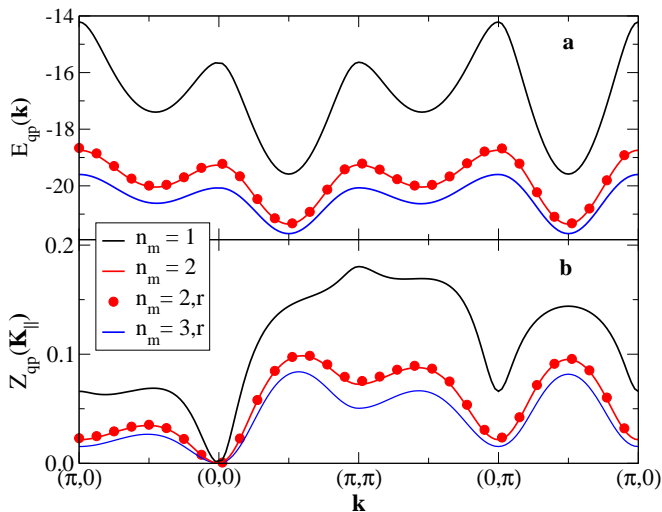


FIG. 2: (a) Quasiparticle dispersion (in units of J_{dd}) along various cuts in the BZ. The results are for the three-band model using $n_m = 1$ (black line), $n_m = 2$ (red line), restricted $n_m = 2$ (red circles) and restricted $n_m = 3$ (blue line) approximations. In the restricted approximations, only configurations with magnons on adjacent sites are included. (b) The corresponding ARPES quasiparticle spectral weights.

The equations for two-magnon propagators link them to other two- and three- , and possibly also to one-magnon propagators, and so on and so forth. While the full set of exact equations of motion can be thus generated, they are impossible to solve exactly.

We introduce a variational solution using the fact that each time a new magnon is created, the energy is increased by (about) $2J_{dd}$ since up to four Cu-Cu bonds become FM. Many-magnon states are thus energetically expensive and unlikely to be significant components of the lowest-energy eigenstates. We define a variational approximation by choosing an integer n_m and setting all propagators with more than n_m magnons to zero. This leads to a manageable (although still infinite) sparse system of equations that can be solved efficiently.

Since ED results show a distortion of the AFM background only rather close to the hole (Fig. 3 of Ref. [15]) it is reasonable to expect that small n_m may already give a good approximation. To check this, we calculate the results for $n_m \leq 3$. For $n_m = 2$ we do both the full variational calculation that allows the magnons to be at any distance from one another, and the restricted calculation where only configurations with the two magnons on adjacent sites are kept (the hole can be located anywhere). In the $n_m = 3$ case we perform only the restricted calculation where the magnons are in a connected cluster. The corresponding dispersions of the low-energy quasiparticle are shown in Fig. 2(a) along several cuts in the full Brillouin zone (FBZ).

The most striking observation is that the dispersions have a shape similar to that measured experimentally,

with deep isotropic minima at $(\frac{\pi}{2}, \frac{\pi}{2})$. This shows that even the very simple $n_m = 1$ solution already captures important aspects of the correct quasiparticle dynamics.

As expected for bigger variational spaces, the dispersions for larger n_m lie at lower energies. The bandwidths for $n_m = 2, 3$ are about half of that for $n_m = 1$, due to standard polaronic physics. Consider $n_m = 2$: while it is energetically favourable for the hole to be near the secondly emitted magnon, as they have antiparallel spins, configurations with the hole near the first magnon are not favorable because of their parallel spins. If the first magnon is bound in the cloud it is in configurations like in Fig. 1(g), where its location limits the number of broken AFM bonds. Alternatively, this magnon can dissociate from the cloud resulting in excited states starting from $E_{1,gs} + 2J_{dd}$, i.e. the ground-state energy of the $n_m = 1$ quasiparticle plus the $2J_{dd}$ cost for a magnon located far from it. For our parameters, this continuum starts at $\approx -17.58J_{dd}$ so the $n_m = 2$ quasiparticle band must become narrower in order to fit below it. The comparison between the full and the restricted $n_m = 2$ cases confirms that the connected magnon clusters (which cost less exchange energy) account for the overwhelming contribution to the low-energy quasiparticle, as expected.

The $n_m = 3, r$ results show an additional narrowing of the bandwidth from $2.6J_{dd}$ for $n_m = 2$, to $2.05J_{dd}$. This solution is thus very close to the $2J_{dd}$ bandwidth of the fully converged case. This is not surprising since the quasiparticle cannot possibly bind too many magnons in its cloud, given that each magnon is at a different location and that the hole can interact with at most one favorable magnon (with antiparallel spin) in any configuration. We conclude that the $n_m = 3, r$ solution is already quantitatively accurate, and indeed its dispersion is in excellent agreement with the ED dispersion of Ref. [15].

This quantitative agreement between the variational and ED results shows that quantum spin fluctuations of the AFM background (fully included in ED but frozen in our variational approach) have little or no effect on the quasiparticle's dynamics. This is because in three-band models the hole can move freely on the O sublattice, so it can easily go to absorb magnons created previously and then emit others at new locations to move the cloud, resulting in fast quasiparticle dynamics. Spin fluctuations of the background, which act on a slower time scale (J_{dd} is the smallest energy) are then not essential for this dynamics. Indeed, we have attempted to gauge the effect of spin fluctuations for $n_m = 2$ by adding in the equations of motion terms that directly link two-magnon and $G_{\beta\alpha}$ propagators, mimicking spin fluctuations that either produce or remove a pair of nn magnons close to the hole. Such terms lead to very minor quantitative changes, as will be reported elsewhere [20].

This conclusion may seem surprising since for one-band models it is believed that spin fluctuations are essential in determining the quasiparticle dispersion: as a ZRS moves

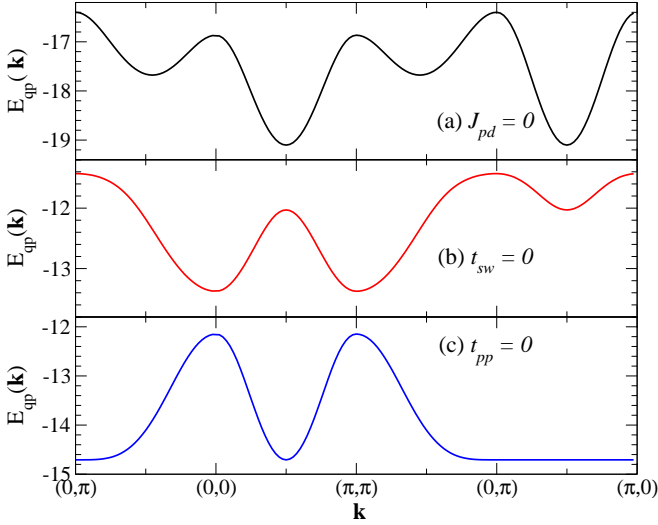


FIG. 3: Quasiparticle dispersion for the three-band model and $n_m = 2$, when we set (a) $J_{pd} = 0$; (b) $t_{sw} = 0$; (c) $t_{pp} = 0$. The other parameters are kept at their stated values.

it creates a string of wrongly oriented spins (magnons) whose energy increases linearly with its length, and which “ties” it near the starting position. In the absence of spin fluctuations, the quasiparticle acquires a finite mass only by executing Trugman loops [18] which are many-step (and thus very slow) processes that lead to a very heavy quasiparticle [19]. Spin fluctuations act faster to remove pairs of nn magnons from the string and thus release the ZRS. These arguments, however, depend essentially on the assumption that only nn hopping of the ZRS is possible, despite the knowledge that the resulting dispersion is wrong, being nearly flat along $(0, \pi) - (\pi, 0)$. To obtain agreement with experiments, second and third nn hopping must be added [9, 11]. These allow the ZRS to move freely on its magnetic sublattice and get away from the string of defects that nn hopping creates, similar to what happens in three-band models. The longer-range hopping thus changes the phenomenology qualitatively and in its presence, we find that spin fluctuations are no longer essential for the quasiparticle dynamics in one-band models either, unlike when only nn hopping is allowed [20].

A natural follow-up question is whether careful tuning of the parameters is needed to achieve this dispersion, or whether this shape is generic. The answer is the latter. Specifically, $\mathcal{H}_{J_{pd}}$ has almost no effect on the shape of $E_{qp}(\mathbf{k})$: even setting $J_{pd} = 0$ leaves it virtually unchanged, only shifting the overall value as exchange energy is lost, see Fig. 3(a). Setting either $t_{sw} = 0$ or $t_{pp} = 0$ leads to very different dispersions (Figs. 3(b), (c)), however if t_{pp} and t_{sw} are comparable, the correct shape appears. In fact, a deep minimum at $(\frac{\pi}{2}, \frac{\pi}{2})$ is then achieved even for $n_m = 0$ (not shown). This confirms the speculation in Ref. [15] that $E_{qp}(\mathbf{k})$ arises through constructive interference between T_{pp} and T_{swap} , and

shows that both terms are needed to properly describe the quasiparticle dynamics. Note that many studies of three-band models ignore T_{pp} or treat it as a perturbation [22–25] (for more discussion, see the supplementary material of Ref. [15]).

Having established that the shape of $E_{qp}(\mathbf{k})$ is robust, we now analyze the quasiparticle ARPES weight. If $\mathbf{K} = (\mathbf{K}_{\parallel}, K_z)$ is the photoelectron’s momentum and ω is the transferred energy, and assuming an unpolarized beam, the ARPES intensity [21] is $A(\mathbf{K}, \omega) \sim \sum_{\mathbf{k}, \mathbf{G}} \delta_{\mathbf{K}_{\parallel} + \mathbf{k}, \mathbf{G}} \sum_{\alpha, \beta} e^{i\mathbf{G} \cdot \mathbf{R}_{\alpha\beta}} \eta_{\alpha\beta} A_{\alpha\beta}(\mathbf{k}, \omega)$. We checked that this gives the correct unfolding if we decouple the hole from the spins, since then the dispersion in the FBZ can be calculated analytically. Here \mathbf{G} are the reciprocal lattice vectors of the MBZ and \mathbf{k} are momenta in the first MBZ. The first sum shows that ARPES detects quasiparticles of quasi-momentum \mathbf{k} equal to the photohole’s in-plane momentum $-\mathbf{K}_{\parallel}$, modulo \mathbf{G} . $\mathbf{R}_{\alpha\beta} = \mathbf{R}_{i,\alpha} - \mathbf{R}_{i,\beta}$ is the distance between the O sites α, β and $A_{\alpha\beta}(\mathbf{k}, \omega) = -\frac{1}{\pi} \text{Im} G_{\alpha\beta}(\mathbf{k}, \omega)$ are the spectral weights of the sublattice propagators. Finally, $\eta_{\alpha\beta} = 1$ if the orbitals α and β are both either $2p_x$ or $2p_y$, and zero otherwise. The quasiparticle ARPES spectral weight, $Z_{qp}(\mathbf{K}_{\parallel})$, is the weight at the energy $\omega = E_{qp}(\mathbf{k})$ of the quasiparticle, *i.e.* $A(\mathbf{K}, \omega \rightarrow E_{qp}(\mathbf{k})) \rightarrow Z_{qp}(\mathbf{K}_{\parallel}) \delta(\omega - E_{qp}(\mathbf{k}))$.

In Fig. 2(b) we plot $Z_{qp}(\mathbf{K}_{\parallel})$ along various cuts in the FBZ. The first observation is that unlike $E_{qp}(\mathbf{k})$, $Z_{qp}(\mathbf{K}_{\parallel})$ does not have MBZ periodicity: the evolution along $(0, 0) - (\pi, \pi)$ is not symmetric about $(\frac{\pi}{2}, \frac{\pi}{2})$. This is expected: while all $A_{\alpha\beta}(\mathbf{k}, \omega)$ must, and indeed do, exhibit MBZ periodicity, $A(\mathbf{K}, \omega)$ does not because of the $e^{i\mathbf{G} \cdot \mathbf{R}_{\alpha\beta}}$ phases. If \mathbf{K}_{\parallel} is inside the first MBZ then $\mathbf{G} = 0$ and, for example, ARPES measures constructive interference between the two $2p_x$ orbitals’ contributions. If \mathbf{K}_{\parallel} crosses into the second MBZ, then $\mathbf{G} = (\pm\pi, \pm\pi)$ and ARPES measures destructive interference between these two orbitals since they are at a distance $(0, a = 1)$ apart.

It is worth pointing out that a similar approach (Néel order plus a few magnons) for one-band models does not lead to any asymmetry. This is because even though there are two sublattice Bloch-states with the ZRS located on either magnetic sublattice, there is no interference between them as they belong to sectors with different total spin S_z . Additional Hubbard and spin-fluctuations corrections must be included to obtain an asymmetric spectral weight, see for example Ref. [26].

The second observation is that $Z_{qp}(\mathbf{K}_{\parallel})$ disagrees along the $(0, 0) - (\pi, \pi)$ cut with the experimental measurements which find large weight near $(\frac{\pi}{2}, \frac{\pi}{2})$ that decreases fast on both sides [9, 13]. (ED predicts $Z_{qp}(\pi, \pi) = 0$ because its quasiparticle has spin $3/2$ in that region. Such an object cannot be fully described with a Néel background which breaks invariance to spin rotations). Since the situation improves with increasing n_m , it is possible that going to higher n_m may fix this problem. However, such an explanation is rather unsatisfactory because it

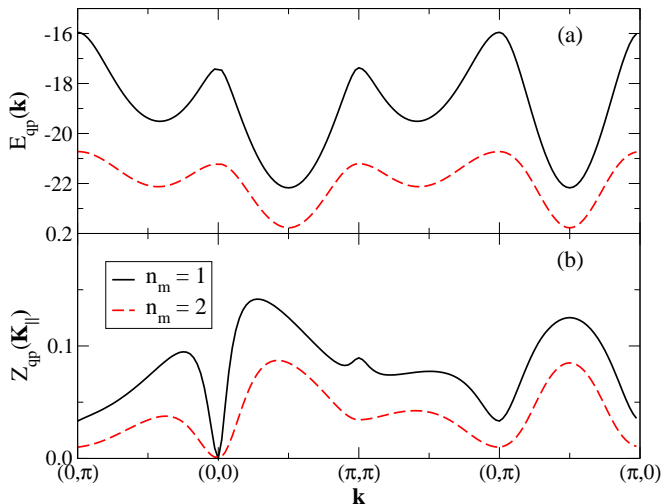


FIG. 4: Same as in Fig. 2, but for the five-band model.

suggests a sensitive dependence of the ARPES weight on the precise structure of the magnon cloud, unlike the robust insensitivity of the dispersion.

To check for an alternative explanation, we add the second set of in-plane O $2p$ orbitals to our model, resulting in the new unit cell sketched in Fig. 1(h). These orbitals are usually ignored because they do not hybridize directly with the Cu $3d_{x^2-y^2}$ orbitals. However, they do hybridize heavily with the ligand $2p$ orbitals occupied by the hole, so their role should be evaluated more carefully and this can be done easily with our method.

For the Hamiltonian, this requires us to expand T_{pp} accordingly. This is achieved without introducing new parameters because nn hopping between two new orbitals also has magnitude t_{pp} , while between new and old orbitals $\tilde{t}_{pp}/t_{pp} = (t_{pp,\sigma} - t_{pp,\pi})/(t_{pp,\sigma} + t_{pp,\pi}) = 0.6$ since $t_{pp,\pi} = t_{pp,\sigma}/4$. We can also add nnn hopping \tilde{t}'_{pp} for the new orbitals. Since $t_{pp,\sigma}$ scales with distance like $1/d^4$, it follows that $\tilde{t}'_{pp} = t_{pp,\sigma}/4 = 0.2t_{pp}$ [27]. This is smaller than $t'_{pp} \approx 0.6t_{pp}$ for the old orbitals for whom nnn hopping is boosted through hybridization with the $4s$ orbital of the bridging Cu. In any event, we find very little sensitivity to the precise values we use for \tilde{t}'_{pp} [20].

We study the five-band model with the same variational approximations; now there are 64 sublattice propagators $G_{\beta\alpha}(\mathbf{k}, \omega)$, leading to a corresponding increase in the number of equations of motion. Fig. 4 shows the quasiparticle dispersion and ARPES spectral weight for the $n_m = 1, 2$ solutions. For $E_{qp}(\mathbf{k})$, the results are very similar to the results shown in Fig. 2(a), but the bands are somewhat wider, as expected because of the increased bare kinetic energy. We have checked that the dependence on J_{pd} , t_{sw} and t_{pp} is essentially unchanged. Indeed, the expectation that this other set of orbitals has little effect on the quasiparticle dynamics is correct.

However, their addition has a significant effect on the

evolution of $Z_{qp}(\mathbf{K}_{\parallel})$ on the $(0,0) - (\pi,\pi)$ cut. The asymmetry is maintained but the results now show a decrease of the ARPES spectral weight on both sides of the MBZ boundary, in agreement with experimental data [9, 13].

The fact that the weight is significantly changed for the five-band model vs. the three-band model even though the dispersion is not much affected should not be a surprise. Since ARPES measures interference between like $2p$ orbitals, the quasiparticle weight can be significantly affected even by rather small redistributions of the wavefunction among orbitals, unlike the energy. These results suggest that a full understanding of the evolution of the spectral weight at low dopings, currently still missing, may require inclusion into theoretical models of these additional orbitals. This will only increase the need for accurate approximations like the one we propose here, since exact numerical approaches become even more challenging to implement in larger Hilbert spaces.

To summarize, we used a simple variational approach to study a quasiparticle in three- and five-band models of an infinite CuO_2 layer, while also being able to gauge accuracy by increasing the variational space. Our results compare well with available results from ED of small clusters. Since the variational approach ignores the effect of spin-fluctuations in the AFM layer, the good agreement for the dispersion strongly supports the idea that these spin fluctuations do not play the important role in the quasiparticle dynamics attributed to them based on results for one-band models with only nn hopping.

This is a very important finding because properly describing the background spin fluctuations is very difficult and a major barrier to studying the two-hole sector to understand the effective interactions between quasiparticles, which is the second piece of knowledge (besides the quasiparticle dispersion) needed in order to propose accurate simple(r) effective models. Our method allows us to distinguish the magnons emitted and absorbed by holes, which are treated exactly, from those due to background fluctuations, which are ignored. Since the method also generalizes to treat few-hole states, we are now able to investigate the role of magnon exchange in mediating strong attractions between holes, and to verify whether this attraction is indeed absent from the currently used one-band effective models, as speculated in Ref. [16]. This work is now in progress.

Acknowledgements: We thank B. Lau and W. Metzner for insightful comments. This work was funded by QML, CIFAR and NSERC.

Competing interests statement: The authors declare no competing financial interests.

[1] Bednorz, J.G. and Müller, K.A. Possible high T_c superconductivity in the Ba - La - Cu - O system. *Z. Phys.*

- B* **64**, 189 (1986).
- [2] Emery, V. J. Theory of high- T_c superconductivity in oxides. *Phys. Rev. Lett.* **58**, 2794 (1987).
 - [3] Zaanen, J., Sawatzky, G. A. and Allen, J. W. Band gaps and electronic structure of transition-metal compounds. *Phys. Rev. Lett.* **55**, 418 (1985).
 - [4] Lee, P.A., Nagaosa, N. and Wen, X-G., Doping a Mott insulator: Physics of high-temperature superconductivity. *Rev. Mod. Phys.* **78**, 17 – 85 (2006).
 - [5] Ogata, M. and Fukuyama, H. The tJ model for the oxide high- T_c superconductors *Rep. Prog. Phys.* **71** 036501 (2008)
 - [6] Lau, B., Berciu, M. and Sawatzky, G.A. Computational approach to a doped antiferromagnet: Correlations between two spin polarons in the lightly doped CuO_2 plane. *Phys. Rev. B* **84**, 165102 (2011).
 - [7] Zhang, F.C. and Rice, T.M. Effective Hamiltonian for the superconducting Cu oxides. *Phys. Rev. B* **37**, 37593761 (1988).
 - [8] Eskes, H. and Sawatzky, G. A. Tendency towards Local Spin Compensation of Holes in the High- T_c Copper Compounds. *Phys. Rev. Lett.* **61**, 1415 (1988).
 - [9] Wells, B.O. *et al.* E versus k Relations and Many Body Effects in the Model Insulating Copper Oxide $\text{Sr}_2\text{CuO}_2\text{Cl}_2$. *Phys. Rev. Lett.* **74**, 964 – 967 (1995).
 - [10] Andersen, O.K., Liechtenstein, A.I., Jepsen, O., and Paulsen, F. LDA energy bands, low-energy hamiltonians, t' , t'' , $t_\perp(k)$, and J_\perp . *J. Phys. Chem. Solids*, **56** 1573 (1995).
 - [11] Leung, P.W., Wells, B.O. and Gooding, R.J. Comparison of 32-site exact-diagonalization results and ARPES spectral functions for the antiferromagnetic insulator $\text{Sr}_2\text{CuO}_2\text{Cl}_2$. *Phys. Rev. B* **56**, 6320 – 6326 (1997).
 - [12] Pavarini, E., Dasgupta, I., Saha-Dasgupta, T., Jepsen, O. and Andersen, O. K. Band-Structure Trend in Hole-Doped Cuprates and Correlation with $T_{c,max}$. *Phys. Rev. Lett.* **87**, 047003 (2001).
 - [13] Damaschelli, A., Hussain, Z. and Shen, Z-X. Angle-resolved photoemission studies of the cuprate superconductors. *Rev. Mod. Phys.* **75**, 473 (2003).
 - [14] Ronning, F. *et al.* Universality of the electronic structure from a half-filled CuO_2 plane. *Phys. Rev. B* **67**, 035113 (2003).
 - [15] Lau, B., Berciu, M. and Sawatzky, G.A. High-Spin Polaron in Lightly Doped CuO_2 Planes. *Phys. Rev. Lett.* **106**, 036401 (2011)
 - [16] Möller, M., Sawatzky, G.A. and Berciu, M. Magnon-Mediated Interactions between Fermions Depend Strongly on the Lattice Structure. *Phys. Rev. Lett.* **108**, 216403 (2012).
 - [17] Berciu, M. Few-particle Green's functions for strongly correlated systems on infinite lattices. *Phys. Rev. Lett.* **107**, 246403 (2011).
 - [18] Trugman, S. A. Interaction of holes in a Hubbard antiferromagnet and high-temperature superconductivity. *Phys. Rev. B* **37**, 1597-1603 (1988).
 - [19] Berciu, M. and Fehske, H. Aharonov-Bohm interference for a hole in a two-dimensional Ising antiferromagnet in a transverse magnetic field. *Phys. Rev. B* **84**, 165104 (2011).
 - [20] Ebrahimnejad, H. and Berciu, M. (to be submitted).
 - [21] Haverkort, M.W., Elfimov, I.S. and Sawatzky, G.A. Electronic structure and self energies of randomly substituted solids using density functional theory and model calculations, arXiv:1109.4036.
 - [22] Emery, V.J. and Reiter, G. Mechanism for high-temperature superconductivity *Phys. Rev. B* **38**, 4547 – 4556 (1988).
 - [23] Frenkel, D.M., Gooding, R.J., Shraiman, B.I. and Siggia, E.D. Ground-state properties of a single oxygen hole in a CuO_2 plane *Phys. Rev. B* **41**, 350 – 370 (1990).
 - [24] Petrov, Y. and Egami, T. Exact-diagonalization study of electron-lattice coupling in the effective two-band tJ model, *Phys. Rev. B* **58**, 9485 – 9491 (1998).
 - [25] Models similar to ours are used in both Zaanen, J. and Oles, A.M. Canonical perturbation theory and the two-band model for high- T_c superconductors *Phys. Rev. B* **37**, 9423 – 9438 (1988); and in Ding, H.-Q., Lang, G.H. and Goddard, III, W.A. Band structure, magnetic fluctuations, and quasiparticle nature of the two-dimensional three-band Hubbard model *Phys. Rev. B* **46**, 14317 – 14320 (1992), however in one-dimension (former) or for a 4×4 cluster (latter).
 - [26] Sushkov, O.P., Sawatzky, G.A., Eder, R. and Eskes, H. Hole photoproduction in insulating copper oxide. *Phys. Rev. B* **56**, 11769 – 11776 (1997).
 - [27] Harrison, W. A. Elementary Electronic Structure (World Scientific, Singapore, 1999).